DOI: 10.15849/IJASCA.230720.20

Int. J. Advance Soft Compu. Appl, Vol. 15, No. 2, July 2023
Print ISSN: 2710-1274, Online ISSN: 2074-8523

Improved Pneumonia Discovery and Classification by Convolutional Neural Network

Salma Hameedi Abdullah

University of Technology, Computer Engineering Department, Iraq, Baghdad
E-mail: Salma.H.Abdullah@uotechnology.edu.iq

Abstract

Training and comparing different images using deep learning techniques play a vital role in image classification. However, these are typically dependent on large scales of datasets and accuracy produced by the models within a certain time. The goal of this paper is to increase accuracy to improve Pneumonia Discovery and Classification by adding batch normalization in a fully connected layer and decreasing processing time by modifying the learning Adam optimizer. The proposed method consists of Convolution neural networks with enhanced fully connected layers and modified learning rate for Adam optimizer to enhance the accuracy and to reduce processing time. Models were trained by passing the input to the different layers of the models. Then the input and concealed (hidden) layer, ReLU is castoff as an initiation function, however, in the production layer softmax is used as a stimulation function which changes the probability distribution of the prediction. For overfitting reduction, dropout is used in individually concealed neurons through 0.5 possibilities. The results were obtained after compiling the model with Adam optimiser for loss function and fitting it with the training and validation datasets. 'Test', 'training', and 'validation' datasets found under 'chest x-ray', consisting of normal class and pneumonia class were used to learn, examine, and legalize the models. Both the proposed models, VGG16 and VGG19, increased the validation accuracy from 87.28% to 98.72% and 88.46 to 92.81% respectively, and the processing time decreased from 30 to 20 ms against a state-of-the-art solution.

Keywords: *Classification, Convolution neural networks (CNN), Deep Learning, pneumonia, 3D images, 2D images, Computed tomography (CT).*

1 Introduction

The most dangerous disease affecting the lungs was pneumonia. Through examining CT scans, X ray images, it can be perceived in the initial phases [1]. It is one of the greatest shared biological infections. Throughout history, viral infections have remained unique in the severe pressures on human fitness [2]. Viral and bacterial infections harm the lungs [3]. Symptoms of pneumonia are common and include pain, coughing, and shortness of breath. Each year 7.7% of the world's populace is hurt from pneumonia. Therefore, early detection of such diseases is critical. With the advent of an automatic medicinal image, the task of

Received 1 April 2023; Accepted 25 June 2023

organisation has expanded meaningfully [4]. This job goal is to identify medicinal images into predefined groups [5]. The request for deep learning prototypes produced further activity in the medical field with the speedy advancement in computer-aided techniques [6] [7]. Deep learning (DL) architecture has shown practical predictive ability and excellent performance with physicians [8]. Multiple tasks have been performed using the DL model for chest radiographs, including identifying tuberculosis [9], segmentation of tuberculosis [10], mass recognition [11], detection of COVID-19 [12] [13], and classification of radiographs [14]. Automatic organisation of chest radiographs by deep learning models is proliferating and selecting a suitable area of interest (ROI) in chest radiographs has been used to detect pneumonia [15]. Additionally, applying DL models avoids the problem that traditional approaches take a long time to find a result. Though models need a great amount of healthy labelled preparation data.

A convolution neural network (CNN) works similarly to the human brain then is cast off to classify complex image arrangement appreciation tasks. CNN requires a smaller number of parameters and connections compared to other neural networks because CNN is preferred for the image classification process. The convolution neural network comprises different hidden and input/output layers, which apply previous knowledge to recognize newer tasks [16]. The pneumonia detection process is performed by the previously mentioned SonoAVC [17]. CNNs containing of contribution, hidden, then production layers, are individual of the generally effective deep-learning techniques in medicinal image examination [18]. A CNN is firstly qualified using a training informations to learn the geographies in the data set. Then be used to aim at similar feature extraction besides classification. CNNs are greatly reliant on many factors, like the excellence of the preparation dataset, the amount of layers castoff in the stimulation function, and the organisation aptitude. The accuracy achieved can be affected by dissimilar reversion and classification victims. Collecting databases and detecting pneumonia with computer-based systems remains challenging, but this leads the development of a simple and effective process. [18] Use a CNN for automated lung detection with an overall f-score of 74.5. I suggested U-net-based segmentation, since the proposed method is in the same field as CNN but guided by a different model proposed by [16].

The proposed method modifies the high-precision solution given by [16]. The proposed method consists of batch normalisation [6] and an improved learning rate of the Adam optimiser [19]. Batch normalisation helps improve the accuracy and variation of the learning rate of the Adam optimiser and reduces processing time.

This paper aims to introduce an automated pneumonia detection system using machine learning. Current manual detection techniques are slow and flawed. Therefore, to make the system fast and automated [19], we collected data on pneumonia and proposed a detection method using CNN. Machine learning will play an essential role in this medical field to ensure maximum accuracy.

This proposed method introduces two proven, highly accurate CNN models with modifications to increase accuracy and reduce time. Batch normalisation is added before ReLU and after fully connected layers to make the model more stable and less error-prone. The learning rate of the Adam optimiser has been changed to ensure faster processing times.

The residual parts of this work are prepared by way of the following. In part 2 interrelated work was illustrated, defines the problem as reported in previous related literature, and Section 3, 'Proposed method', and details the block diagram and the projected method. This is followed by, Section 4, 'Results', which describes numerous testing methods used in this procedure. Lastly, Section 5, 'Deductions and Forthcoming Work', compares the consequences of the projected method then presents the paper's conclusions.

2 Related Work

The authors of this study [19] produced a public database on follicles in ovaries that required AI support to enhance the accuracy of image recognition on this large dataset. The 3D-DWT-based algorithms showed an overall score of 78, which is slightly better than other baseline algorithms; however, the limited number of datasets and independent rates proved to be the limitation of this method. But different CNN methods can be used to improve the detection techniques [19].

Moreover, in [16], to reduce the number of deaths due to pneumonia, the writers planned a method that used convolutional neural networks. The planned model achieved, respectively, an accuracy of 85.6% and 92.31%, which is an improved accuracy. The limiting factor of this method was the lack of spatial invariance. To achieve full accuracy, the work used deep learning and transfer learning.

In addition, [20] proposed a better method to classify thyroid nodules using CNN rather than the surgical way of using the biopsy, which can harm the patient. The proposed model showed 91.6% accuracy, which is better than the current classified-based approach. The limited number of datasets was an issue when classifying the thyroid nodules. The use of generator and descriptor networks described here can be applied in other research to improve the results of CNN.

Another study, [21], applied deep learning techniques associated with CNNs to subdivide gastritis patients into subtypes (A, B, and C). The overall accuracy obtained by this method was 84%, and the associated sensitivity and specificity were found to be high for type B at 100% and 93%, respectively. The dataset needed to be appropriately optimised. CNN accuracy for classification can be improved by using an optimiser.

An additional study, [22], introduced an automatic pneumonia detection technique and identification method for hair loss to detect the problem in 30 minutes. This method is faster and safer with only an 11.8% error rate, which is better than the manual detection technique. This study could have been improved loss functions and activation functions.

In [23] planned a DL model that takes the relative of bone construction into the semantic separation of bone SPECT image to detect SPECT bone early. The model achieved a rate of 0.992, 0.772, 0.678, and 0.610 for PA (correctness), CPA (Exactness), Rec (Recollection), and IoU, respectively; however, the study was limited by an insufficient number of samples. These deep-learning techniques could advance the use of SPECT bone segmentation for early detection.

Further work [24] has improved detection techniques for early-stage pharyngeal patients using deep learning methods. The solution proposed by the author has an understanding of 85.6%, which is upper than the result found through white bright imaging (70%). Images of complex structures and narrow spaces in the pharynx mislead the diagnosis, so more

images of regularly shaped structures would allow the model to perform better. Using more images from cancer patients to train the data could improve the performance of datasets in CNN algorithms, and the same process could be applied to different medical fields in the future.

The authors in [25] apparently trained and validated the different CNNs with a tile of datasets. The proposed method correlates the gene with phenotypes giving high accuracy using a CNN. Furthermore, with approved algorithms, they obtain 92-95%; however, further research in this area is complicated due to limited datasets. The results can be improved by adding a loss function and applying more data sets.

The proposed system in the next study was a significant benchmark in deep learning as it passed the human expert's level of accuracy of ROI selection. The score produced by the system was 0.582, which was the highest ever compared to the manual system. Quantitative analysis was done correctly. Deep learning techniques with MF-CNN algorithms are used to make the scoring of breast cancer detection automatic [26].

In [27], a solution was proposed to find a temperature-aided solution for the identification of thyroid nodules in their early stages using deep learning techniques. The proposed solution indicated that the temperature difference can detect the presence of thyroid nodules in the neck. It cannot predict these nodules for obese people. Temperature analysis using CNN is a benchmark in the area of CNN networks.

In [28], the authors proposed a method for the classification of lung cancer by using deep learning techniques, with the proposed method classified using subtypes such as ADC and SqCC. The analysis ignored other possible subtypes of lung cancer, like carcinoma.

In another study, a new method was applied that used 50 layers for the purpose of detecting diseases of the skeletal system. The authors achieved 90% in sensitivity and specificity. The sensitivity and specificity did not increase as expected because only static images were used [29].

In [6], a solution was proposed that provides a new time series-based method to detect hypertension in its early stages by analysing electrocardiographic Holter signals. The model showed excellent results by giving an accuracy of 98%; however, because a large number of parameters were used, the models took a long time to train the data. This shows that the proposed model has a high potential for evolution in the medical field to detect hypertension in its early stages.

In [30], the solution provides a reasonable way to use deep learning and convolutional neural networks for automatic recognition in knee joint classification. The solution increases the accuracy level by more than 10% compared to the present methods of observations by doctors or the use of artificial intelligence. The snake method leads to an increased accuracy level and provides a slow execution speed. This solution makes more knowledgeable discoveries for automatic recognition and health care.

3 The State of the Art

In figure 1, the scattered blue line shows the better topographies, and the scattered red line shows the limitations of the current state of the art within the field of a suggested CNN-

based pneumonia detection system [16]. Numerous CNNs were educated to categorise x-ray images into pneumonia class and non-pneumonia class, with a number of convolutional layers and changing different hyperparameters. In the paper, six models have been declared. The first and second models contain two and three convolutional layers, respectively. The other four models are pre-trained models, which are VGG16, VGG19, ResNet50, and Inception-v3. The proposed process has two stages: pre-processing and processing of data.

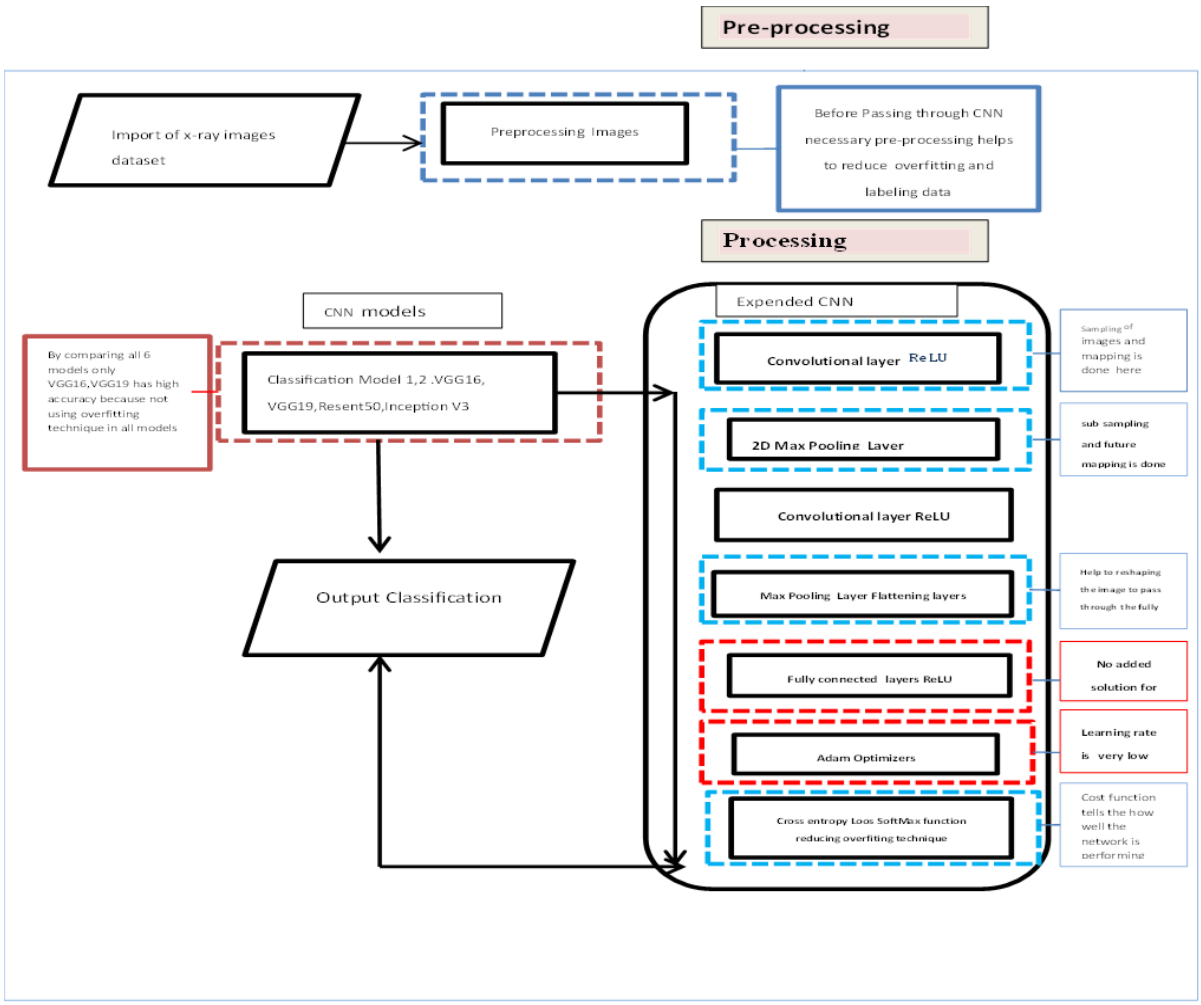

Fig.1. State-of-the-art diagram [16].

3.1 Pre-processing

The proposed state-of-the-art diagram has two phases: pre-processing and processing. Data is imported from Kaggle in this step. The imported data is passed through the pre-processing block before passing through the CNN [16].

3.2 Dataset

In Kaggle, a dataset below the designation as Chest X-Ray Images. The dataset holds 5216 imageries for preparation and 624 imageries for testing. Image details are 64 x 64

grayscale images. There are three types of images in the dataset, including, ‘normal’, ‘bacterial pneumonia’, and ‘viral pneumonia’.

3.3 Processing

The CNN architecture was proposed in [16] to train and classify the pre-processed data. The proposed CNN prototypical can assist in reducing the number of deaths due to phenomena. It is the best solution because the author implemented all the processes properly here. The process steps used in the convolution models are described in the following sections.

3.3.1 Convolutional Layer

This layer first transforms the input images into matrix form and maps the features of images. To make processing easier, the layer reduces the size of the images. The size reduction led to the loss of features, but the feature detector retained essential features of the images. In the first convolution layer, multiple feature detectors achieve multiple feature maps.

3.3.2 Activation Function

The author [16] proposed two types of activation functions. ReLU and softmax are the activation functions used in the work. ReLU (Rectified linear function) is a widely used activation function. The ReLU gives output 1 when the input is positive; otherwise, it gives 0. ReLU performs better than other activation functions like sigmoid or tanh avoiding and rectifying vanishing gradient problems. The ReLU function is represented by f(x) given as:

$$f(x) = max(0,x) \qquad (1)$$

The additional activation function softmax normalises the inputs and logits to the possibility distribution function. The output of the last layer is logits. In the last layer of the CNN, softmax is used with a cost function.

3.3.3 Combining (pooling) layer

This layer decreases the scopes of the contribution images while performing the down sampling of images. Two different methods are max pooling and average pooling. Max pooling selects the value with the highest pixel using the feature detector from the window's 'Max' function. It assistances models recognise the salient topographies of the images. Average pooling is additional method that computes the middling value of the window calculated by the feature detector.

3.3.4 Flattening layers and fully connected layers

The flattening layer helps to procedure the piece maps of pooled images. Afterward the flattening layer, the images are nourished into the completely associated layer, which makes the prediction. The cost function can be calculated depending on the prediction, which is guided by the cross-entropy loss function. To optimise the models, the Adam optimiser has been used. The Adam optimiser is useful when training a large number of datasets.

3.3.5 Reducing Overfitting

Dropout is used to reduce model overfitting. Every hidden layer's output with a probability of 0 drops out at 0.

Limitations: The limitation of the models in [16] is that there is no added solution for data standardization and error reduction, which can be improved by adding batch normalisation. The Adam optimiser is selected with a larger learning rate value, which causes an increase in training time.

3.4 State of the art Mathematical Equation

Given output for fully connected layer in [16] is given as:

$$y_{fc} = w * x + b \quad (1)$$

Where,

y_{conv} is the output from fully connected block.
W is the masses of the parameter.
x is the contribution sequence and b bias.

In [16], the ReLU function was applied with the production of completely connected layer and the production after ReLU is given as:

$$y = ReLU(y_{conv}) \quad (2)$$

Here, y is the output after applying ReLU function.

The ReLU function is given as,

$$f(x) = max(0,x) \quad (3)$$

$f(x)$ is the output of ReLU.

max is the maximum value function which takes input x. This function will set all positive values to 1 and all negatives to 0.

In [16], a model training method was provided using Adam optimiser:

$$\alpha_t = \begin{cases} \alpha_0 & 0 < t <= 100 \\ \alpha_0 * 5 & 100 <= t <= 300 \end{cases} \quad (4)$$

Here, α_t is the training rate with t number of iterations.

α_0 is the learning rate. The value of $\alpha_0 = 0.001$ is very low, and it will take longer training time.

In [16], cost function was provided as cross entropy loss and is given by:

$$CrossEntropyLoss = -(ylog(p) + (1-y)log(p)) \quad (5)$$

Here, y represents binary pointer (0 or 1)

p is a forecast possibility.

The softmax purpose proposed by Jain et al. (2020) is denoted by s and is given by:

$$s(z)_i = \frac{e^{z_i}}{\sum_{j=1}^{k} e^{z_j}} \quad (6)$$

s= softmax

Z was a contribution vector

e^{z_i} was a standard exponential function for contribution

K was Quantity of groups in multiclass cataloguing

e^{z_j} Was a standard exponential function for production.

In [16], a reducing overfitting technique was used:

$$Reducing\ Overfitting = Dropout \quad (7)$$

Here, dropout assigns 0 to each hidden Neuron of the output with 0.5 probability.

3.5 Algorithm for the state of the art

Step 1: Beginning

Step 2: Import the one image from Kaggle

Step 3: Pre-processing the images (removing noises and labelling images)

*Step 4: Passing image into convolution Layer with ReLU activation function (64 * 64 image and 32 feature maps)*

Step 5: Pass the output of the previous layer into 2D max pooling layer

Step 6: Input images into the convolution layer with the ReLU activation function (64 feature maps)

Step 7: Pass the production of the previous layer into the 2D max pooling layer

Step 8: Again, pass through the convolute layer for model 2 (128 feature maps), which is again conceded through the 2D max pooling layer and then trodden

Step 9: Pass the preceding layer's output into the completely associated layer (256 perceptron) with ReLU as an activation function.

Step 10: Compile the model with loss function as an Adam optimiser and SoftMax as an activation function.

Step 11: End

4 The Proposed Method

The proposed model has two stages with pre-processing stage and a processing stage. In the best solution [16], the authors used six models of CNN to compare the results and used multilayer CNN. The second-best solution is the proposed selection with different information and a higher accuracy model [6]. The author introduced a batch normalisation technique in the fully connected layer of CNN, which helps to standardize and reduce classification errors. The projected solution has different correctness and enhanced time [6] taken as the third-best solution. The author proposed an improved learning rate for Adam optimiser, which helps reduce the time taken for data training [4]. The proposed system has two phases: pre-processing and processing. Data is imported from Kaggle in this step. The imported data is passed through the pre-processing block before passing through the convolutional network CNN to calculate the classified output. It must go through different input, hidden, and output layers. Data is passed through the same CNN architecture proposed by [4], the first complication layer, max pooling layer, complication layer, max pooling layer, flattening, and fully connected layer guided by ReLU as an activation function. Moreover, those are compiled with the Adam optimiser for the loss function and softmax as a beginning function. The given prototypical is modified through using the batch normalisation technique given by [6], which helps stabilize and reduce classification errors. Furthermore, the loss function is modified by using the higher learning rate given by [6].

4. 1 Proposed Mathematical Equation

In [19], the output of fully connected layer is given as:

$$y_{bn} = BN(y_{fc}) \quad (8)$$

Where,

y_{bn} is the output from batch normalization.

y_{fc} is the production of completely connected layer.
Batch normalization helps to standardize the input and accelerate the training.

In [19], the stimulation function ReLU castoff in the production of batch normalization is shown as:

$$y = ReLU(y_{bn}) \quad (9)$$

Here, y is the output after adding ReLU and batch normalization.

The modified function after adding batch normalization is:

$$Mf(x) = BN(y_{fc}) \quad (10)$$

Here,

$Mf(x)$ is the modified batch normalization function.

y_{fc} is the production of completely connected layer.

The modified output after applying ReLU and Batch Normalization is,

$$My = ReLU(Mf(x)) \quad (11)$$

So, modified output from ReLU is given as,

My is the output of modified ReLU function with adding batch normalization.

Bu et al., (2020) provided the Adam algorithms with training rate as:

$$\alpha_t = \begin{cases} \alpha_0 & 0 < t <= 100 \\ \alpha_0 * 5 & 100 <= t <= 300 \end{cases} \quad (12)$$

Here,

the value of α_0= 0.002 which is a slightly higher learning rate.
This will improve training time periods by reducing the time.

The improved Adam optimiser is proposed as:

$$M\alpha_t = \begin{cases} M\alpha_0 & 0 < t <= 100 \\ M\alpha_0 * 5 & 100 <= t <= 300 \end{cases} \quad (13)$$

Here,

$M\alpha_t$ is modified training rate with t number of iterations.

$M\alpha_0$is known as the modified learning rate with the value of 0.002.

The output of enhanced classification for detection pneumonia is given as:

$$ECC = CrossEntropyLoss + My + M\alpha_t + \text{softmax} + \text{dropout} \quad (14)$$

Here,

ECC is the enhanced classification output and My is the output of modified ReLU function after adding batch normalization. $M\alpha_t$ is the modified learning rate for Adam optimiser. Softmax is the stimulation function castoff in the productivity layer and dropout is the technique for reducing overfitting.

Batch normalisation with a convolution layer provides the extra solution to stabilise the process and reduce errors. Error reduction is the way to improve network accuracy. The state of the art's best solution should have included any stabilisation techniques that can effectively improve the model's accuracy. The preliminary wisdom rate of the Adam optimiser is modified, which helps to process time improve. The learning rate taken in the state-of-the-art's greatest resolution was shallow, which needs to take a large number of epochs, and causes a longer processing time. The proposed figure is given as:

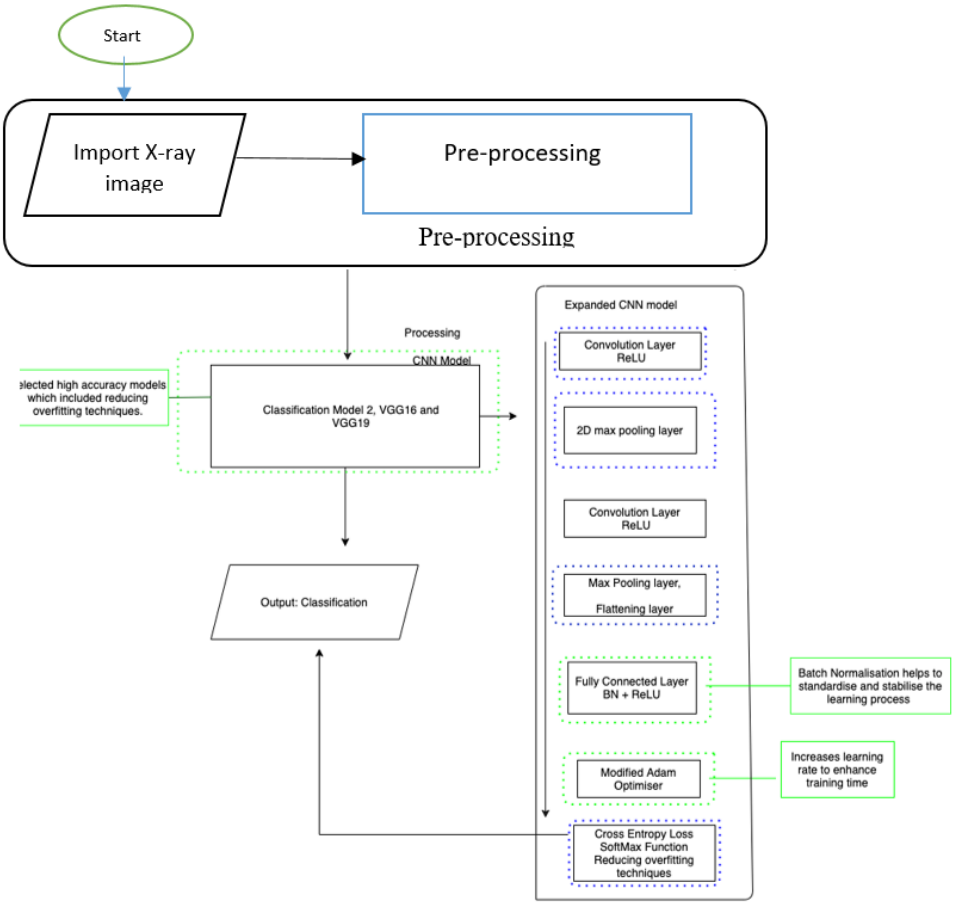

Fig 2. Proposed scheme diagram.

4.2 Algorithm of projected method

Step 1: Begin

Step 2: Import the one image from Kaggle

Step 3: Pre-processing the images (removing noises and labelling images)

*Step 4: Pass image into convolution Layer with ReLU activation function (64 * 64 image and 32 feature maps)*

Step 5: Pass the output of the previous layer into 2D max pooling layer

Step 6: Input images into the convolution layer with the ReLU activation function (64 feature maps)

Step 7: Pass the production of the previous layer into the 2D max combining layer

Step 8: Again, pass through the convolute layer for model 2. (128 feature maps) which is again conceded through the 2D max combining layer and then flattened

Step 9: Pass the previous layer's output into the fully connected layer (256 perceptrons) with ReLU as an activation function.

Step 10: Compile the model with loss function as an Adam optimiser and softmax as an activation function.

Step 11: End

5 Results

The proposed model used Tensorflow and Keras to implement 5216 training and 624 test images [16]. The proposed methods used the same number of datasets used in state-of-the-art solutions. The resolution of the planned formal of the art was processed in Mac OS laptops using the code editor Jupyter Notebook.

The testing process is taken step by step for the proposed method which enables a user to see the images of chest X-rays of regular patients and images of chest x-ray of abnormal patients.

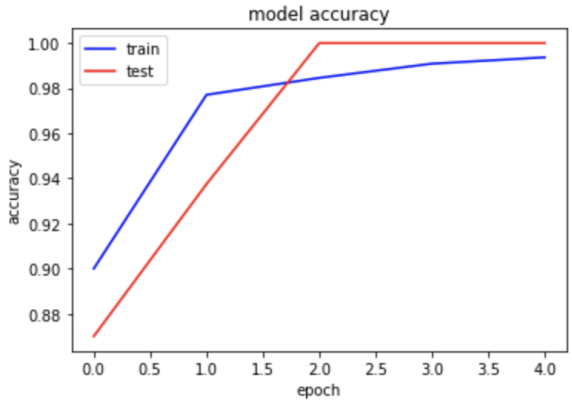

Fig.3. Model accuracy of the vgg16 model with comparison to the epoch given in different steps of the proposed state-of-the-art solution can be seen between training and test data. The blue line of the graphs shows the accuracy of training datasets, and the red line shows the accuracy of test datasets in the above graph.

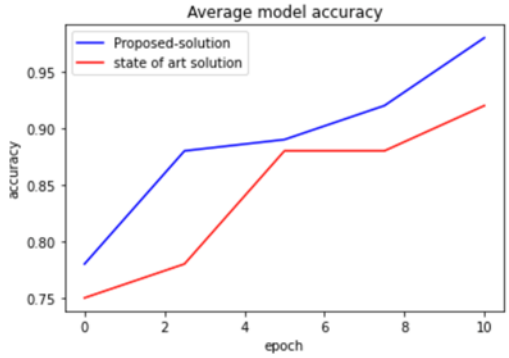

Fig.4 Comparison average model accuracy of VGG16 model of the state-of-the-art and proposed solutions. The model accuracy between the two models is plotted with accuracy in each epoch. Here, the blue line of the graphs represents proposed solution accuracy over each step, and the red line shows the state-of-the-art solution's correctness over each epoch.

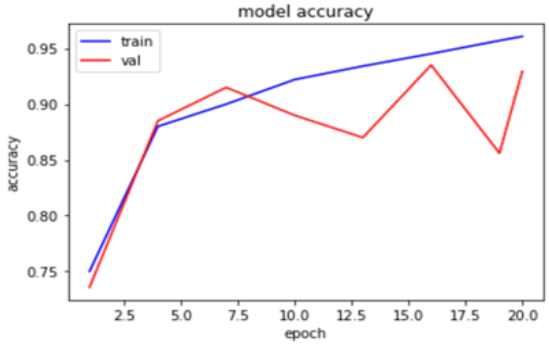

Fig.5. Models accuracy of VGG19 models of the proposed solution is shown above. VGG19 models with improved methods show an increase in accuracy over epochs. The red line in the graphs represents the changing value of validation data over epochs. The blue line represents the changing value of training data over epochs.

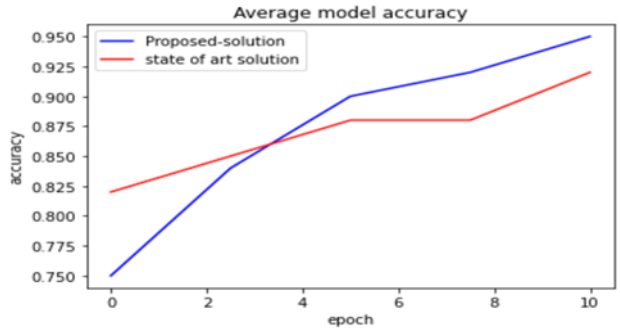

Fig. 6. The above figure represents the model's accuracy of VGG19 models comparing proposed solution model's accuracy with the state-of-the-art solution over changing epochs. The blue line represents the increase in model accuracy of the projected

explanation, whereas the red line signifies the correctness increase in the state-of-the-art model explanation

Table1. Accuracy recall and f-value of state-of-the-art models

Name Model	Accuracy	Recall	F1-score
VGG16	87.17%	92%	91%
VGG19	88.45%	94%	92%

Table2. Accuracy recall and f-value of the proposed method

Name Model	Accuracy	Recall	F1-score
VGG16	98.91%	99%	96%
VGG19	92.8%	98%	94%

6 Discussion

The proposed solution shows that accuracy can be improved significantly by additional stabilisation and error decrease techniques. The modified algorithms of VGG16 models showed an accuracy of 98.72%, which is 10% more than the state-of-the-art solution. The solution of the proposed VGG19 model shows an accuracy of 92.81%, which is 4% more than the state-of-the-art solution. However, there is no significant decrease in processing time. Both the models take 8 hours to train the data with only a 1-3 second difference. The value of both the state-of-the-art solution and the proposed method is carried out by implementing both methods and plotting those into graphs. The completely associated layer's stability improved, and the error rate was reduced which helped to advance the complete accuracy. The enhancement of a completely associated layer with the addition of batch normalisation plays a vital role in developing the model's overall performance. The learning rate with an Adam optimiser reduction also helped to reduce processing time in small amounts. Overall, the addition of batch normalisation and an increase in the learning rate helped improve the system's accuracy.

For creating CNN models to classify images, continuous improvement is going on in different methods to reduce errors and increase accuracy. Here, the proposed methods successfully improved the overall accuracy of the models with a 10% increase in the accuracy of VGG16 from a state-of-the-art solution and a 4% increase in the accuracy of VGG19 from a state-of-the-art solution. This research also reduced the processing time by 3 seconds by changing the learning rate. Additionally, these new features increase the image's detection rate by increasing the models' accuracy. The contrast concerning the proposed method and state-of-the-art solutions is shown in Table 3.

Table 3: Contrast between the planned method and state-of-the-art solutions

	Proposed Solution	State of Art Solution
Name of the solution	Batch Normalisation and Improved Adam optimiser	No solution for stabilisation than Adam optimizer through a higher learning rate
Accuracy	Accuracy will be improved by reducing the error rate and stabilising the classification.	No added solution for stabilisation, which causes lower accuracy.
Processing Time	As the value of the learning rate is introduced to 0.001 the training time will be reduced for the optimiser, resulting in a reduction of processing time.	Given the learning rate of 0.002, causing a longer time to train and process.
Contribution 1	Adding the batch normalisation in fully connected layer before ReLU. $Mf(x) = BN(y_{fc})$ (10) Which results an, $My = ReLU(Mf(x))$ (11)	The state of art solution has no stabilisation technique and is given by, $y = ReLU(y_{conv})$ (2)
Contribution 2	Changing the learning rate in Adam optimiser, $M\alpha_t = \begin{cases} M\alpha_0 & 0 < t <= 100 \\ M\alpha_0 * 5 & 100 <= t <= 300 \end{cases}$ (13) $M\alpha_0$ is the modified learning rate with a value of 0.002	$\alpha_t = \begin{cases} \alpha_0 & 0 < t <= 100 \\ \alpha_0 * 5 & 100 <= t <= 300 \end{cases}$ (4) $\alpha_0 = 0.001$ Which is very low, and it will take longer training time.

7 Conclusion and Future Works

The proposed solution with image detection techniques includes an entirely new feature in the state-of-the-art solution from the second-best solution. The included batch normalisation techniques significantly increase the model's overall accuracy in both models compared to the solution of the state of the art. The techniques give additional stabilisation methods for the proposed solution and reduce the error of the models. The minimisation of error and stabilisation of networks plays a vital role in improving the model's accuracy, as mentioned in the second-best solution. The proposed methods increased accuracy by 10 and 4% in VGG16 and VGG19, which is more than the expected outcome.

Using all the improved methods, the proposed method has been tested in TensorFlow and Jupyter Notebook by implementing third-party libraries in python like Keras, Pandas and MATLAB. Along with this, the proposed solution helped to visualize the data effectively with test and validation datasets.

Instead of increasing the learning rate in Adam optimiser, future research needs to find lower processing time in lower epochs and lower initial learning rate. Here, the research is done in 2D datasets, and future research needs to be done in 3D. Along with it, future research needs to be done on a PC with a powerful processor, which would help to minimize the processing time..

References

[1] P. Jeyaraj and E. R. S. Nadar, "Computer-assisted medical image classification for early diagnosis of oral cancer employing deep learning algorithm," Journal of Cancer Research and Clinical Oncology, vol. 145, no. 4, pp. 1-9, 2019.

[2] Ortiz-Toro, C.; García-Pedrero, A.; Lillo-Saavedra, M.; Gonzalo-Martín, C, (2022). Automatic pneumonia detection in chest X-ray images using textural features. Comput. Biol. Med. 2022, 145, 105466.

[3] Ben Atitallah, S.; Driss, M.; Boulila, W.; Koubaa, A.; Ben Ghezala, H. Fusion of convolutional neural networks based on Dempster–Shafer theory for automatic pneumonia detection from chest X-ray images. Int. J. Imaging Syst. Technol. 2022, 32, 658–672.

[4] Wang, L.; Wang, H.; Huang, Y.; Yan, B.; Chang, Z.; Liu, Z.; Zhao, M.; Cui, L.; Song, J.; Li, F. Trends in the application of deep learning networks in medical image analysis: Evolution between 2012 and 2020. Eur. J. Radiol. 2022, 146, 110069.

[5] Singhal, A.; Phogat, M.; Kumar, D.; Kumar, A.; Dahiya, M.; Shrivastava, VK Study of deep learning techniques for medical image analysis: A review. Mater. Today Proc. 2022, 56, 209–214.

[6] Potočnik, B., Munda, J., Reljič, M., Rakić, K., Knez, J., & Vlaisavljević, V. et al. (2020). Public database for validation of follicle detection algorithms on 3D ultrasound images of ovaries. Computer Methods And Programs In Biomedicine, 196, 105621. https://doi.org/10.1016/j.cmpb.2020.105621.

[7] Y. Xiao, J. Wu, Z. Lin, and X. Zhao, "A deep learning-based multi-model ensemble method for cancer prediction," Computer Methods and Programs in Biomedicine, vol. 153, no. C, pp. 1-9, 2018.

[8] Salahuddin, Z.; Woodruff, H.C.; Chatterjee, A.; Lambin, P. Transparency of deep neural networks for medical image analysis: A review of interpretability methods. Comput. Biol. Med. 2022, 140, 105111.

[9] Kale, S.P.; Patil, J.; Kshirsagar, A.; Bendre, V. Early Lungs Tuberculosis Detection Using Deep Learning. In Intelligent Sustainable Systems; Springer: New York, NY, USA, 2022; pp. 287–294.

[10] Bellens, S.; Probst, G.M.; Janssens, M.; Vandewalle, P.; Dewulf, W. Evaluating conventional and deep learning segmentation for fast X-ray CT porosity measurements of polymer laser sintered AM parts. Polym. Test. 2022, 110, 107540.

[11] Zhang, L.; Mueller, R. Large-scale recognition of natural landmarks with deep learning based on biomimetic sonar echoes. Bioinspir. Biomimetics 2022, 17, 026011.

[12] Le Dinh, T.; Lee, S.H.; Kwon, S.G.; Kwon, K.R. COVID-19 Chest X-ray Classification and Severity Assessment Using Convolutional and Transformer Neural Networks. Appl. Sci. 2022, 12, 4861. [CrossRef]

[13] Sajun, A.R.; Zualkernan, I.; Sankalpa, D. Investigating the Performance of FixMatch for COVID-19 Detection in Chest X-rays. Appl. Sci. 2022, 12, 4694.

[14] Furtado, A.; Andrade, L.; Frias, D.; Maia, T.; Badaró, R.; Nascimento, E.G.S. Deep Learning Applied to Chest Radiograph Classification—A COVID-19 Pneumonia Experience. Appl. Sci. 2022, 12, 3712.

[15] Malhotra, P.; Gupta, S.; Koundal, D.; Zaguia, A.; Kaur, M.; Lee, H.N. Deep Learning-Based Computer-Aided Pneumothorax Detection Using Chest X-ray Images. Sensors 2022, 22, 2278.

[16] Jain, R., Nagrath, P., Kataria, G., Sirish Kaushik, V., & Jude Hemanth, D. (2020). Pneumonia detection in chest X-ray images using convolutional neural networks and transfer learning. Measurement, 165, 108046. https://doi.org/10.1016/j.measurement.2020.108046.

[17] Khan, A., Sohail, A., Zahoora, U., & Qureshi, A. (2020). A survey of the recent architectures of deep convolutional neural networks. Artificial Intelligence Review, 53(8), 5455-5516. https://doi.org/10.1007/s10462-020-09825-6.

[18] Iori, M.; Di Castelnuovo, C.; Verzellesi, L.; Meglioli, G.; Lippolis, D.G.; Nitrosi, A.; Monelli, F.; Besutti, G.; Trojani, V.; Bertolini, M.; et al (2022) . Mortality prediction of COVID-19 patients using radiomic and neural network features extracted from a wide chest X-ray sample size: A robust approach for different medical imbalanced scenarios. Appl. Sci. 2022, 12, 3903.

[19] Paragliola.G, & Coronato.A, (2020).An hybrid ECG-based deep network for the early identification of high-risk to major cardiovascular events for hypertension patients, Journal of Biomedical Informatics,Volume 113, January 2021, 103648, https://doi.org/10.1016/j.jbi.2020.103648.

[20] Shi, G., Wang, J., Qiang, Y., Yang, X., Zhao, J., Hao, R., Yang, W., Du, Q. and Kazihise, N., 2020. Knowledge-guided synthetic medical image adversarial augmentation for ultrasonography thyroid nodule classification. Computer Methods and Programs in Biomedicine, 196, p.105611.https://doi.org/10.1016/j.cmpb.2020.105611.

[21] Kundu R, Das R, Geem ZW, Han GT, Sarkar R (2021) Pneumonia detection in chest X-ray images using an ensemble of deep learning models. PLOS ONE 16(9): e0256630. https://doi.org/10.1371/journal.pone.0256630.

[22] Urban, G., Feil, N., Csuka, E., Hashemi, K., Ekelem, C., & Choi, F. et al. (2020). Combining Deep Learning With Optical Coherence Tomography Imaging to

Determine Scalp Hair and Pneumonia Counts. Lasers In Surgery And Medicine. https://doi.org/10.1002/lsm.23324.

[23] Lin, Q., Luo, M., Gao, R., Li, T., Man, Z., Cao, Y., & Wang, H. (2020). Deep learning based automatic segmentation of metastasis hotspots in thorax bone SPECT images. PLOS ONE, 15(12), e0243253. https://doi.org/10.1371/journal.pone.0243253.

[24] Tamashiro, A., Yoshio, T., Ishiyama, A., Tsuchida, T., Hijikata, K., & Yoshimizu, S. et al. (2020). Artificial intelligence-based detection of pharyngeal cancer using convolutional neural networks. Digestive Endoscopy, 32(7), 1057-1065. https://doi-org.ezproxy.csu.edu.au/10.1111/den.13653.

[25] Badea, L., & Stănescu, E. (2020). Identifying transcriptomic correlates of histology using deep learning. PLOS ONE, 15(11), e0242858. https://doi.org/10.1371/journal.pone.0242858.

[26] Wahab, N., & Khan, A. (2020). Multifaceted fused-CNN based scoring of breast cancer whole-slide histopathology images. Applied Soft Computing, 97, 106808. https://www.sciencedirect.com/science/article/abs/pii/S1568494620307468?via%3Dihub.

[27] Damião, C., Montero, J., Moran, M., da Cruz Filho, R., Fontes, C., Lima, G., & Conci, A. (2020). On the possibility of using temperature to aid in thyroid nodule investigation. Scientific Reports, 10(1). https://www.nature.com/articles/s41598-020-78047-1.

[28] Bicakci, M., Ayyildiz, O., Aydin, Z., Basturk, A., Karacavus, S., & Yilmaz, B. (2020). Metabolic Imaging Based Sub-Classification of Lung Cancer. IEEE Access, 8, 218470-218476. https://ieeexplore-ieee-org.ezproxy.csu.edu.au/document/9270569.

[29] Guo, L., Gong, H., Wang, Q., Zhang, Q., Tong, H., & Li, J. et al. (2020). Detection of multiple lesions of gastrointestinal tract for endoscopy using artificial intelligence model: a pilot study. Surgical Endoscopy. https://link-springer-com.ezproxy.csu.edu.au/article/10.1007/s00464-020-08150-x.

[30] Steinbuss, G., Kriegsmann, K. and Kriegsmann, M., 2020. Identification of Gastritis Subtypes by Convolutional Neuronal Networks on Histological Images of Antrum and Corpus Biopsies. International Journal of Molecular Sciences, 21(18), p.6652. http://dx.doi.org.ezproxy.csu.edu.au/10.3390/ijms21186652.

Notes on contributors

Dr. Salma Hameedi Abdullah is currently a lecturer at the faculty of Computer Engineering Department, University of Technology, Iraq. She obtained her Ph.D. in computer vision from the University of Technology in 2018. Her research interest includes computer vision, deep learning, internet of things (IoT), and pattern recognition. She can be contacted at email: Salma.H.Abdullah@uotechnology.edu.iq